EVALUATING CARDIAC GENE EXPRESSION IN MATERNAL PHENYLKETONURIA OFFSPRING

A Thesis by

Jennifer Ellie McCoy

Bachelor of Science, Wichita State University, 2002

Submitted to the College of Liberal Arts and Sciences
and the faculty of the Graduate School of
Wichita State University in partial fulfillment of
the requirements for the degree of
Master of Science

May 2006

EVALUATING CARDIAC GENE EXPRESSION IN MATERNAL PHENYLKETONURIA OFFSPRING

I have examined the final copy of this Thesis for form and content and recommend that it be accepted in partial fulfillment of the requirement for the degree of Master of Science with a major in Biological Sciences.

_____
J. David McDonald, Committee Chair

We have read this thesis and recommend
its acceptance:

_____
William J. Hendry III, Committee Member

_____
Jeffrey May, Committee Member

_____
James Bann, Committee Member

ACKNOWLEDGEMENTS

I sincerely thank my mentor, Dr. McDonald, for all the time and effort he has invested in my undergraduate *and* graduate education. My decision to pursue graduate studies at WSU was largely influenced by the opportunity to continue gaining research knowledge from Dr. McDonald. Thanks for putting up with me for all these years! I would also like to thank my committee members: Dr. Hendry, Dr. May, and Dr. Bann. Your willingness to answer my questions (and share your equipment) made it possible for me to finish my research. I must thank Dr. Brown for patiently helping me with statistical analysis. My gratitude also goes to Dr. Jia, for his many consultation sessions on sequence alignments, primer design, and Endnotes.

I thank Kathy Dandurand and Fawn Beckman, not only for taking care of the animals used in this study, but also for their friendship. I am grateful to Ellie Skokan for her guidance, and for being a terrific female role model in science for me. I must also thank Isabel Hendry and Dr. Shuai, for helping me trouble shoot several aspects of my research. Your input was invaluable to me. I thank Darren Francisco for his incessant willingness to help me with all my stupid computer problems. And I owe Maria Russell many, *many* margaritas for her constant help and support, both professionally and personally. I would not have finished my research and writing on time without her help in devising a plan to meet these deadlines.

Finally, I can't forget my brother Michael, the artist/graphic designer extraordinaire. Thanks for always listening to me practice my scientific presentations, even though you don't understand what the hell I'm talking about!

ABSTRACT

Maternal phenylketonuria (MPKU) is a teratogenic syndrome, caused by development of offspring in a uterine environment made toxic by the metabolic imbalance of PKU. The birth defects resulting from untreated MPKU include microcephaly with concomitant mental retardation, growth retardation, and congenital heart defects. Congenital heart defects have been identified and characterized in MPKU offspring, using the BTBR-*PAH*^{enu2} mouse MPKU model. Subsequently, this mouse model was used to start investigating the molecular basis of MPKU congenital heart defects. It was determined that three genes involved in heart contractility and development were significantly downregulated in MPKU fetal hearts at 18.5 days postcoitum, compared to non-PKU control offspring. These three genes were troponin T2 (*Tnnt2*), troponin I3 (*Tnni3*), and ryanodine receptor 2 (*Ryr2*).

We used the BTBR-*PAH*^{enu2} mouse model to further evaluate the relationship between maternal hyperphenylalaninemia and cardiac gene expression in MPKU fetal hearts. It was hypothesized that an association exists between maternal blood phenylalanine (Phe) levels and expression levels of certain cardiac genes. More specifically, our alternate hypothesis stated that elevated maternal blood Phe levels are associated with decreased expression of *Tnnt2*, *Tnni3*, and *Ryr2* in MPKU fetal hearts. Relative quantification of *Tnnt2*, *Tnni3*, and *Ryr2* transcript abundance in MPKU fetal hearts was performed using real-time PCR. Linear regression analysis was then performed on relative *Tnnt2*, *Tnni3*, and *Ryr2* transcript levels as a function of maternal blood Phe concentration. The regression analyses for all three genes were found to be nonsignificant. Therefore, we were unable to reject the null hypothesis, which stated that

there is no association between maternal blood Phe levels and the abundance of *Tnnt2*, *Tnni3*, and *Ryr2* transcripts in MPKU fetal hearts.

TABLE OF CONTENTS

LIST OF TABLES

LIST OF FIGURES

LIST OF ABBREVIATIONS

bp	Base pair
c-	Cardiac
C-	Carboxyl
cDNA	Complimentary DNA
CICR	Calcium-induced calcium release
C_T	Critical threshold
dpc	Days postcoitum
ENU	*N*-ethyl-*N*-nitrosurea
EDTA	Ethylenediaminetetraacetic acid
g	Gravity
GAPDH	Glyceraldehyde-3-phosphate dehydrogenase gene
HMBS	Hydroxymethyl-bilane synthase gene
kb	Kilobase
kDa	KiloDalton
LNAA	Large neutral amino acids
L-type	Long-lasting calcium current
MPKU	Maternal phenylketonuria
mRNA	Messenger RNA
N-	Amino-
PAGE	Polyacrylamide Gel Electrophoresis
Pah	Phenylalanine hydroxylase gene
PAH	Phenylalanine hydroxylase protein

LIST OF ABBREVIATIONS CONTINUED

Phe	Phenylalanine
PKU	Phenylketonuria
r^2	Coefficient of determination
RNase	Ribonuclease
rRNA	Ribosomal RNA
RT	Reverse transcription
RyR2	Ryanodine receptor 2 gene, cardiac
Ryr2	Ryanodine receptor 2 protein
SDHA	Succinate dehydrogenase complex subunit A gene
ss	Slow-twitch skeletal
T_m	Melting temperature
TnC	Troponin C protein
TnI	Troponin I protein
Tnnc1	Troponin C gene, cardiac
Tnni3	Troponin I gene, cardiac
Tnnt2	Troponin T gene, cardiac
TnT	Troponin T protein
Tris	Tris(hydroxymethyl)aminomethane
Tyr	Tyrosine

LIST OF SYMBOLS

^{o}	degree
μ	micron
Δ	the change in

LITERATURE REVIEW

Phenylketonuria

Phenylketonuria (PKU, McKusick No. 261600) is a metabolic disorder resulting from deficiency of the hepatic enzyme phenylalanine hydroxylase (PAH, EC 1.14.16.1). PAH is responsible for converting the amino acid phenylalanine (Phe) to tyrosine (Tyr). PAH deficiency results in elevated Phe levels in the blood and tissues (1), as well as deficient Tyr levels (2). The clinical features of untreated PKU include mental retardation, hypopigmentation, microcephaly, eczema, epilepsy, and behavioral disturbances (3). PKU is inherited in an autosomal recessive manner; therefore, PKU children are typically born to asymptomatic carrier parents. PKU offspring are not at risk prenatally, since the mother exclusively metabolizes excess Phe; the pathology of PKU only accrues if the PKU child remains untreated postnatally.

PKU results from mutation in the phenylalanine hydroxylase gene (*Pah*), which is located on human chromosome 12q24.1 (4). The *Pah* gene spans 90 kb, contains 13 exons, produces a 2.4 kb long mature mRNA, and encodes a protein 452 amino acids in length (5). Exon 7 encodes the PAH active site; it is frequently mutated in human PKU. A vast array of *Pah* mutations has been documented in humans, and these mutations vary in phenotypic severity. There is an indirect relationship between the amount of residual PAH activity and severity of the disease phenotype (6). Blood Phe concentrations range from 58-120 μM in normal adults. In untreated individuals with classical PKU (defined biochemically as having less than 5% residual PAH activity), blood Phe concentrations as high as 2,400 μM have been observed (7, 8).

When present at high concentrations, Phe becomes toxic to the central nervous system. One reason is because the large neutral amino acids (LNAAs) share a common transporter at the blood-brain barrier. It is thought that, when these LNAA transporters become saturated with Phe, the brain becomes deficient in other LNAAs such as valine, leucine, isoleucine, threonine, histidine, tryptophan, methionine, and tyrosine (9). The resulting imbalance of LNAAs can impair the synthesis of proteins and neurotransmitters, which ultimately affects brain development and function. For instance, production of the neurotransmitter dopamine is dependent on the availability of the precursor amino acid Tyr. Tyr deficiency in PKU hinders dopamine production, which ultimately has an adverse affect on brain development and function (10). This Tyr deficiency in the brain is only exacerbated by saturation of the LNAA transporters at the blood-brain barrier.

In 1951, it was proposed that a low Phe diet might be used as therapy for PKU (11). It was soon discovered that, if dietary treatment was started immediately after birth and adhered to thereafter, PKU children showed normal brain development as well as normal blood Phe levels (12-14). Because of the great importance of beginning treatment shortly after birth, PKU screening in newborns began in 1961. By 1966, PKU screening was mandatory in the majority of the United States. Diagnostic screening for PKU, in conjunction with Phe-restricted dietary guidelines, produced a generation of normally-developed PKU males and females. As these PKU women reached reproductive age, however, a related syndrome called maternal PKU soon developed into an international health problem.

Maternal Phenylketonuria

Maternal PKU (MPKU) is a teratogenic syndrome caused by development of offspring in a uterine environment made toxic by the metabolic imbalance of PKU. The likelihood of fetal damage from maternal PKU can be reduced, but not entirely eliminated, when a Phe-restricted diet is initiated before conception and maintained throughout pregnancy (15). Unless maternal Phe levels are strictly controlled throughout MPKU pregnancy, severe fetal abnormalities occur at a much higher frequency than in non-PKU pregnancies. These abnormalities include, in order of incidence: microcephaly with concomitant mental retardation, intrauterine growth retardation, and congenital heart defects (16, 17).

Congenital heart defects have been reported in approximately 14% of human maternal PKU offspring (18). The risk of congenital heart defects significantly increases when maternal blood Phe levels are greater than 900 μM and when metabolic control is not achieved by the eighth gestational week (19). However, even when metabolic control of maternal blood Phe levels (<600 μM) is maintained throughout pregnancy, approximately 6% of MPKU offspring display heart defects (20). By comparison, the national incidence population rate for congenital heart defects is less than 1% (21). The cardiac defects most frequently seen in MPKU offspring are coarctation of the aorta, tetralogy of Fallot, and hypoplastic left heart syndrome (19).

A portion of the aorta is narrowed in aortic coarctation, thereby restricting blood flow. Surgery is usually advised during infancy to repair this vascular defect. Tetralogy of Fallot consists of four cardiovascular abnormalities: a ventricular septal defect, pulmonary stenosis, hypertrophy of the right ventricle, and an overriding aorta.

Tetralogy of Fallot results in decreased blood flow to the lungs, in addition to mixing of blood from each side of the heart. This cardiovascular defect can also be treated surgically. Usually, a temporary operation is initially performed; complete surgical repair follows later in childhood. In hypoplastic left heart syndrome, the structures on the left side of the heart (including the left ventricle, mitral valve, aortic valve, and some of the aorta) are severely underdeveloped. This defect typically results in extremely low blood flow throughout the body. Hypoplastic left heart syndrome is fatal within the first few days of life unless treated. Treatment is possible through heart transplantation, or in some cases, through a series of operations.

Mouse Model for Phenylketonuria

The BTBR-*PAH*^{enu2} mouse model of PKU was produced through random germline point mutagenesis with *N*-ethyl-*N*-nitrosurea (ENU) (22). This mouse line contains a missense mutation in exon 7 of the *Pah* locus (23). It exhibits the classical PKU phenotype, cognitive deficits, and hypopigmentation (22, 24). The BTBR-*PAH*^{enu2} mouse model has also been shown to model MPKU (25, 26). MPKU offspring from this model demonstrate microcephaly, reduced birth weight, decreased body length, and cardiovascular defects. In addition, a dose-response relationship has been established between maternal blood Phe levels and morphometric parameters of birth defects in offspring from this model.

An assortment of cardiovascular defects was observed in fetal offspring (14.5-19.5 days postcoitum) from hyperphenylalaninemic BTBR-*PAH*^{enu2} females. Abnormalities were seen in the range of 27-46% of the progeny in each litter. Although most defects detected in this study were vascular in nature, some primary heart defects

were also noted. Further, great variation was seen in the types and severities of defects. Abnormalities were noticed in the patterning, size, and absence of various vascular components.

In a previous study using the BTBR-*PAH*^{enu2} mouse model, microarray analysis was used to examine gene expression levels in MPKU fetal hearts at 18.5 days postcoitum (dpc). The analysis showed 1,354 genes with differential expression between control and MPKU hearts (27). The expression of 716 genes was upregulated, while 638 genes were downregulated. Most of these genes had an expression ratio difference less than one fold; however, seventeen genes involved in heart development or contractility showed significant (three fold or greater) reduction in expression. Troponin T2 (*Tnnt2*), troponin I3 (*Tnni3*), and ryanodine receptor 2 (*Ryr2*) were among these seventeen genes; they were chosen for further analysis due to their known roles in cardiac contractility and development. Semi-quantitative real-time PCR confirmed that these three genes were significantly downregulated in the hearts of 18.5 dpc MPKU offspring compared to non-PKU control offspring. Western blots were then performed on the protein fraction from the pooled fetal hearts. The results showed significant reductions in the levels of cardiac Troponin T2 (cTnT) and cardiac Troponin I (cTnI) in fetal MPKU hearts compared to control.

Despite the obvious difference in size, the anatomy of the murine heart and human heart is remarkably similar throughout development (28). The sequence of events which leads to the development of a four-chambered heart from a linear heart tube is analogous between the two species. Therefore, the mouse is frequently used as a model for studying heart development. It is important to note, however, that some of the

developmental events which are complete in the human heart at parturition are still in progress in the heart of the neonatal mouse. Due to this and other slight variations, some caution should be used when comparing human development to a mouse model.

Biomechanical Forces Involved in Heart Morphogenesis

The linear heart tube is formed on embryonic day 8 of murine development and on embryonic day 21 of human development (29, 30). Cardiomyocytes initiate the heartbeat during the late period of heart tube formation (31). All subsequent steps of heart morphogenesis (looping, chamber development, and septation) occur in the presence of biomechanical forces. "These forces include wall shear stress (friction caused by moving blood next to the heart wall), transmural pressure (fluid pressure exerted against the walls due to contraction and relaxation of the heart muscle), and circumferential stretch (cyclical distention of the cardiac tissues resulting from pulsatile blood flow)" (31). These biomechanical forces affect the remodeling and morphogenesis of the developing heart, and thus form a link between heart function and heart development. There is more than one possible mechanism by which this could occur. The mechanical forces of the heart might directly push cells into their appropriate locations. Localized mechanical forces might also affect signaling pathways in the myocardium and endocardium, thereby altering cellular development.

Studies in zebrafish have shown an association between defects in myocardial function and structural heart defects (32, 33). Furthermore, alterations in myocardial gene expression were noted in *silent-heart* zebrafish when the mechanical force of cardiomyocyte beating was absent (34). Since biomechanical forces are required for normal heart development, genes involved primarily in regulating cardiac muscle

contraction also play a secondary, yet crucial, role in guiding proper heart development. These genes encode regulatory proteins such as troponin and tropomyosin, which modulate the interaction of the contractile proteins (actin and myosin) in cardiomyocytes.

Troponin Complex

The troponin complex is involved in the Ca^{2+} regulation of muscle contraction, through its association with actin in the thin filaments of sarcomeres. Muscle contraction is initiated when the cytoplasmic Ca^{2+} threshold is reached. Ca^{2+} binds to the troponin complex and changes its conformation; this shifts tropomyosin away from myosin binding sites on the actin filaments, thus allowing cross-bridge activity. As shown in Figure 1, the troponin complex is composed of three subunits: Troponin C (TnC), Troponin I (TnI), and Troponin T (TnT) (35).

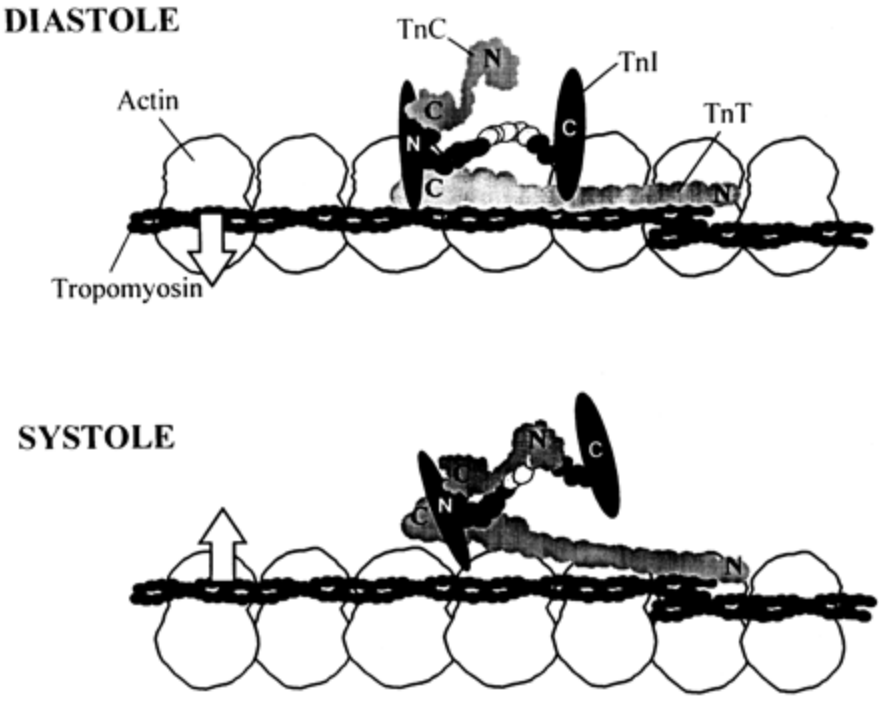

Figure 1. Structure and arrangement of cardiac myofilament proteins in diastole and systole. (36)

TnC is the Ca^{2+} sensitive subunit of the troponin complex, which contains three Ca^{2+} binding sites (37). The binding of Ca^{2+} to TnC induces a steric shift in the troponin complex, which ultimately results in cross-bridge activity. TnC has a molecular weight of 18kDa and contains globular domains at both the C-terminus and N-terminus; it belongs to the helix-loop-helix calcium binding protein family (38).

TnI is the inhibitory subunit of the troponin complex, which prevents muscle contraction in the absence of Ca^{2+}. TnI binds to actin in the relaxed state, thus inhibiting the ATPase activity of actomyosin. TnI has a molecular weight of 24-26.5kDa, and its N-terminus contains a phosphorylation site; cross-bridge activity is less likely to occur when TnI is phosphorylated (38, 39).

TnT binds to tropomyosin and actin, thereby attaching the troponin complex to the thin filament (38). TnT has a molecular weight of 37-39 kDa; phosphorylations sites are contained on both the C-terminus and N-terminus (38, 40). The binding sites for TnI and TnC are found at the globular C-terminal domain, while the binding site for tropomyosin is found at the N-terminus (38, 41).

The subunits of the troponin complex exist in various isoforms, which are encoded by distinct genes (38). These isoforms (slow-twitch skeletal, fast-twitch skeletal, and cardiac) are unique in amino acid sequence as well as structure (42, 43). The isoform(s) expressed depend(s) on the tissue of origin, as well as the developmental stage of the organism (44). The main isoforms found in cardiac muscle are cTnT (translated from *Tnnt2*), cTnI (translated from *Tnni3*), and c/ssTnC (translated from *Tnnc1*). However, skeletal isoforms of TnT, TnI, and TnC are also expressed in the fetal heart (38, 45, 46).

The *Tnnt2* primary RNA transcript is alternatively spliced in the mammalian heart, thus producing four cTnT variants: $cTnT_1$-$cTnT_4$ (45). $cTnT_1$, $cTnT_2$, and $cTnT_4$ are expressed in the fetal heart. $cTnT_3$ is the predominant form in the adult heart; however, $cTnT_4$ is also expressed in the failing human heart.

Tnnt2 mutations in humans account for approximately 15% of familial hypertrophic cardiomyopathies (47). *Tnnt2* missense mutations, which alter the biophysical properties of cTnT, have also been linked to pathogenic cardiovascular remodeling in transgenic mice (47, 48). The *Tnnt2* knockout phenotype has been studied in *silent-heart* zebrafish embryos, which carry a noncoding mutation in *Tnnt2*. Without cTnT, the cardiac sarcomeres do not assemble; this results in a non-contractile heart phenotype (34). Interestingly, myocardial cells from *silent-heart* zebrafish embryos also show significant reductions in tropomyosin and cTnI levels. This suggests the presence of a feedback mechanism to regulate the levels of these sarcomeric proteins.

The necessity of cTnI for survival was observed in *Tnni3* knockout mice (49). These mice developed normally past gestation due to the presence of fetal troponin I isoform (ssTnI) in the heart. However, the expression of the ssTnI began declining 15 days after birth, and the *Tnni3* knockout mice died of acute heart failure on embryonic day 18.

Ryanodine Receptor

The cardiac ryanodine receptor (Ryr2) is encoded by the *RyR2* gene, which is located on human chromosome 1q42-q43 (50). This gene spans 790 kb, contains 105 exons, and encodes a massive, 565 kDa protein (51, 52). Ryr2 proteins are assembled into tetramers to create functional calcium-induced calcium release (CICR) channels;

these channels are located in the sarcoplasmic reticulum of cardiomyocytes, as shown in Figure 2. Electrical excitation of the sarcolemmal membrane activates L-type calcium channels, which produce small increases in Ca^{2+} concentration near Ryr2 channels. This subsequently triggers the opening of Ryr2 channels, resulting in massive influxes of Ca^{2+} from the sarcoplasmic reticulum into the cytoplasm (53). Ca^{2+} then binds to TnC, resulting in cross-bridge activity and cardiac muscle contraction.

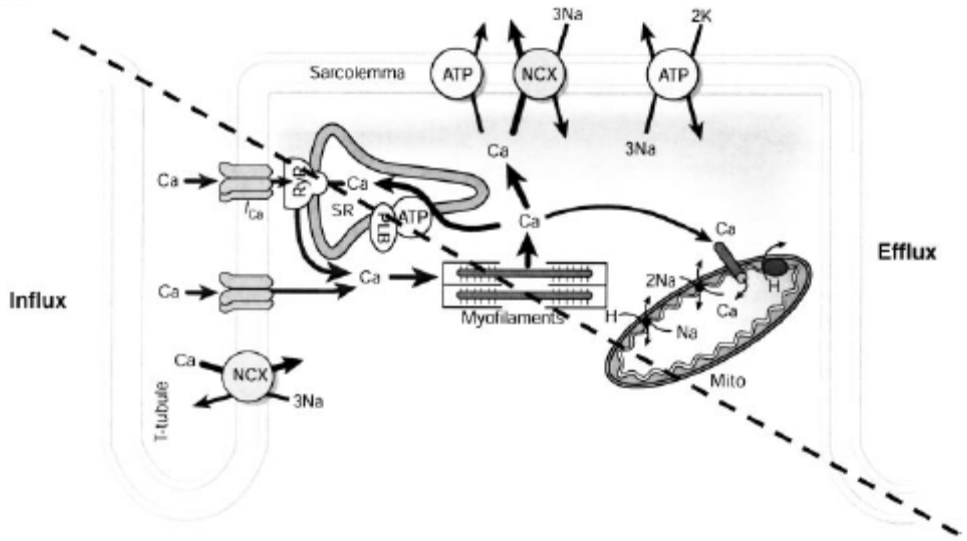

Figure 2. Cardiac excitation-contraction coupling events. (54)
(SR, sarcoplasmic reticulum; Ryr, ryanodine receptor; NCK, Na^{+}/Ca^{2+} exchanger; PLB, phospholamban; Mito, mitochondria)

Although Ryr2 participates in calcium signaling during excitation-contraction coupling in the adult heart, its principle role in the embryonic heart is maintaining cellular Ca^{2+} homeostasis in the developing sarcoplasmic reticulum. *Ryr2* knockout mice developed large vacuolated sarcoplasmic reticulum and structurally abnormal mitochondria; they ultimately died on embryonic day 10 with morphological heart tube

abnormalities (55). In humans, catecholaminergic polymorphic ventricular tachycardia (CPVT) can result from missense mutations within the *RyR2* gene (56).

Goal of Study

A dose-response relationship has been observed for many birth defects resulting from MPKU: these include cognitive ability, microcephaly, and intrauterine growth retardation (57, 58). In addition, it has previously been shown that three genes involved in heart contractility and development (*Tnnt2*, *Tnni3*, and *Ryr2*) are significantly downregulated in the hearts of 18.5 dpc MPKU offspring compared to non-PKU control offspring. The goal of this study is to begin evaluating the relationship between maternal hyperphenylalaninemia and cardiac gene expression in MPKU offspring. It was hypothesized that an association exists between maternal blood Phe levels and the expression of certain cardiac genes. More specifically, the alternate hypothesis states elevated maternal blood Phe levels are associated with decreased expression of *Tnnt2*, *Tnni3*, and *Ryr2* in MPKU fetal hearts. Linear regression analysis was performed on normalized *Tnnt2*, *Tnni3*, and *Ryr2* transcript levels as a function of maternal blood Phe level. This was done to test the null hypothesis, which states no association between maternal blood Phe levels and the abundance of *Tnnt2*, *Tnni3*, and *Ryr2* transcripts in MPKU fetal hearts.

MATERIALS AND METHODS

Experimental Design

The BTBR-*Pah*^{enu2} mice used for this study were obtained from an inbred colony maintained by Dr. McDonald in the animal holding facilities of Wichita State University. This facility is accredited by the American Association for the Accreditation of Laboratory Animal Care, and the project was approved by the Wichita State University Institutional Animal Care and Use Committee. The mice were housed in polycarbonate microisolator cages, maintained under constant environmental conditions, and allowed free access to water and Lab Diet #5001. While in mating cages, the females were pre-conditioned to eat Lab Diet # 5001 in powdered form.

Litters for this study were generated by mating homozygous mutant (*Pah*^{enu2}/ *Pah*^{enu2}) females to heterozygous (*Pah*^{enu2}/ +) males. Females were checked daily before noon for the presence of copulation plugs. As is typical for timed mating experiments in the laboratory mouse, noon on the day of plug detection was designated as 0.5 days postcoitum (0.5 dpc). If a copulatory plug was detected, the female was weighed, given a tail bleed (for determination of pre-treatment maternal blood Phe concentration), and assigned to a particular LNAA dietary treatment condition.

For this study, the LNAA dietary supplement was used to modulate maternal blood Phe levels, as shown previously with this mouse line (59). The composition of the LNAA supplement is shown in Table 1. Several LNAA supplementation levels were utilized, in an effort to produce the range of maternal blood Phe levels necessary to evaluate dose-response. Table 2 shows the dietary conditions each treatment class was exposed to throughout gestation. The powdered LNAA supplement was incorporated

into powdered Purina Rodent Diet # 5001 until a homogenous mixture was formed. This made it impossible for the females to avoid consuming LNAA with their daily food intake.

Table 1. Amino acid composition of LNAA dietary supplement.

Amino Acid	Concentration (μM)
L-Tyrosine	896.2
L-Tryptophan	207.9
L-Methionine	178.6
L-Isoleucine	184.4
L-Leucine	825.1
L-Threonine	223.7
L-Histidine	161.1
L-Lysine	171.1
L-Arginine	143.6
L-Valine	249.3

Table 2. Dietary treatments administered to gestating homozygous mutant BTBR-*Pah*^{enu2} females.

Treatment Group	LNAA Dietary Supplement (daily/animal)	Purina Rodent Diet # 5001 (daily/animal)	Total g diet (daily/animal)
0% LNAA	0 g	6.0 g	6.0 g
16.7% LNAA	1.0 g	5.0 g	6.0 g
20.0% LNAA	1.2 g	4.8 g	6.0 g
33.4% LNAA	2.00 g	4.0 g	6.0 g

Mating pairs were not separated immediately, in case the first mating failed to result in pregnancy. Therefore, each female continued to be checked daily for copulation plugs. A mid-gestational tail bleed was performed at 10.5 dpc, and the female was once again weighed. When pregnancy was visually confirmed (usually around 12 dpc), the female was transferred to a separate cage. Any indication of health abnormality in the female (vaginal bleeding, ill appearance, spontaneous abortion) was noted throughout the

pregnancy. Necropsy was conducted at 18.5 dpc, which is one day before normal murine parturition.

The pregnant female was euthanized by CO_2 asphyxiation for five minutes prior to necropsy. The abdominal cavity was then opened to expose the uterine horns. Fetuses were excised one at a time, starting with the ovarian end of the left uterine horn and working toward the cervical end. The right uterine horn was then emptied, starting once again at the ovary end and moving toward the cervical end. Fetuses were assigned identification numbers to denote their exact position in the left or right uterine horn. Each fetus was weighed on an analytical scale; a blood sample was then collected from the left carotid artery with a microhematocrit capillary tube. The fetus was then separated into head, trunk, and tail portions. Each tissue portion was placed in a separate cryogenic tube and flash frozen immediately in liquid nitrogen. Following excision of the fetuses, a maternal blood sample was collected from the descending aorta with a microhematocrit capillary tube. After collection, the blood specimens were transferred onto filter paper and allowed to dry for subsequent determination of blood Phe determination.

Fetal and maternal blood Phe concentrations were determined by spectrofluorometric assay with the Neonatal Phenylalanine Test Kit (PerkinElmer Life Sciences Inc.). This assay quantitatively measures phenylalanine in the presence of other amino acids (60, 61). Phenylalanine and ninhydrin react in the presence of L-leucyl-L-alanine to create the fluorescent compound 5-(O-Carboxyphenyl)-5-hydroxy-3-phenyl-1-(leucyl-alanine)-2-pyrrolin-4-one. This compound has an excitation wavelength of 390 nm and an emission wavelength of 486 nm. A standard curve of known Phe

concentrations versus fluorescence was generated from each spectrofluorometric assay using the method of least squares line-fitting. The standard curve was then utilized to calculate the blood Phe concentrations of maternal and fetal blood samples within the assay group.

The fetal trunks were stored at -80^{o}C prior to heart isolation. In order to obtain sufficient RNA for analysis, fetal hearts were pooled within litters. The fetal trunks were thawed on wet ice for approximately one hour before heart isolation was performed. One by one, the trunks were submerged in ice cold 1x phosphate buffered saline. Using a dissecting microscope, the chest cavities were opened; the hearts and adjoining vasculature were then excised. Hearts from the same litter were pooled in one ml of Tri Reagent (Molecular Research Center, Inc.). Once heart isolation was complete for the entire litter, an analytical scale was used to determine the pooled tissue weight. Homogenization was then performed using the Ultra-Turrax Tissuemizer (Tekmar).

RNA Isolation Protocol

The single-step method for total RNA isolation was performed using the Tri Reagent protocol (62). Tri Reagent was chosen since the presence of phenol and guanidine thiocyanate in a mono-phase solution inhibits the activity of RNases. The tissue homogenate (50-100 mg of fetal heart tissue homogenized in one ml Tri Reagent) was centrifuged at 4^{o}C for 10 minutes at 12,000 x *g* to pellet any insoluble material. The supernatant was then collected and transferred to a new tube. Following a five minute incubation at room temperature, 100 µl of 1-bromo-3-chloropropane (BCP) was added to the homogenate. The mixture was vortexed vigorously for 15 seconds, incubated at room temperature for 15 minutes, and subsequently centrifuged at 4 ^{o}C for 15 minutes at

12,000 x *g*. Centrifugation separated the mixture into a lower organic phase, an interphase, and an upper aqueous phase. RNA resided exclusively in the aqueous phase, while DNA and proteins were located in the interphase and organic phase.

Approximately 75% of the aqueous phase (450 µl) was transferred to a new RNase-free tube, and 500 µl of isopropanol was added to precipitate the RNA. The mixture was incubated at room temperature for 10 minutes. Following centrifugation at 4 ^{o}C for 8 minutes at 12,000 x *g*, a white RNA pellet was visible. The supernatant was removed from the RNA pellet, and the pellet was vortexed in one ml of 75% ethanol. Afterwards, the mixture was centrifuged at 4 ^{o}C for five minutes at 7,500 x *g*. The ethanol was decanted, and the pellet was air dried for 10-15 minutes.

The pellet was sufficiently dry for resuspension when it began changing color from white to translucent. At this point, the RNA pellet was dissolved in 0.75 µl of pH 8.0 Tris-EDTA buffer (10mM Tris-Cl, pH 8.0 and 1mM EDTA, pH 8.0) per mg tissue. To aid resuspension, the solution was passed through a pipette several times and incubated at 60 ^{o}C for 15 minutes. Absorption spectroscopy was subsequently performed using the Eppendorf Biophotometer to determine RNA concentration and purity. Absorbance values at 230, 260, 280, and 320 nm were assessed to determine RNA purity. Samples were titered to 1.00 µg/µl RNA with pH 8.0 Tris-EDTA buffer following RNA quantification.

Reverse Transcription Protocol

Single-stranded cDNA was created from total cardiac RNA using the Promega Reverse Transcription System. Promega's Reverse Transcription Protocol was followed, except that 2.00 µg total RNA were added to each reaction instead of 1.00 µg total RNA.

In order to denature any secondary RNA structures, the RNA was incubated at 70 °C for ten minutes; the RNA was then transferred to wet ice. The reaction mixture was assembled on wet ice as shown in Table 3. Following assembly, the reaction tubes were incubated at 22 °C for 10 minutes, 42 °C for 15 minutes, 95 °C for 5 minutes, and 0 °C for 5 minutes. Finally, 80 µl of pH 8.0 Tris-EDTA buffer was added to create a final volume of 100 µl.

Table 3. Reverse transcription reaction components.

Component	[stock]	[working]	µL/reaction
Nuclease-Free H_20	n/a	n/a	7.75
$MgCl_2$	25 mM	5 mM	4.00
Reverse Transcription Buffer	10x	1x	2.00
dNTPs	10 mM	1 mM	2.00
RNasin Ribonuclease Inhibitor	40 u/µl	1 u/µl	0.50
AMV Reverse Transcriptase	20 u/µl	7.5 u/µg RNA	0.75
Random Hexamer Primers	0.5 µg/µl	25 ng/µl	1.00
Total RNA	1.00 µg/µl	100 ng/µl	2.00
Total Volume			20.00

Real-Time PCR: An Overview

Real-time PCR allows for the detection of PCR amplification levels during the exponential phase of PCR (63). The number of PCR products should precisely double during each cycle of this phase; for this reason, there is a quantitative relationship between the initial amount of target molecules and the quantity of PCR products formed. The accumulation of PCR products is detected in real-time, using a reporter which emits fluorescence when bound to the PCR products. When the fluorescence intensity of the PCR reaction reaches a predetermined level of fluorescence, the critical threshold (C_T) value is assigned. This C_T values indicates the number of PCR cycles required for a

given reaction to reach the fluorescence threshold. There is an inverse relationship between the initial number of target molecules present and the resulting C_T value.

Once C_T has been determined, a melting curve is generated to determine the melting peak (T_m) of the PCR products. Analysis of the melting curve yields information about the identity and purity of the PCR products. If the T_m value generated corresponds to the predetermined T_m value of the desired PCR product, no additional processing of the sample is required.

Absolute quantification assays interpolate the exact number of initial target molecules from a standard curve. Although this method is more costly and time consuming, it is preferred when attempting to measure small-fold changes in gene expression. Alternately, relative quantification assays verify differences in gene expression without placing exact numerical values on them. The C_T value of the target gene is normalized to the C_T value of an internal control gene. A unitless number is generated, which can be used to compare the relative amounts of target molecules in different samples. Relative quantification is less costly and less time consuming; however, small fold changes in gene expression can be missed.

Real-Time PCR Protocol

Relative quantification of *Tnnt2*, *Tnni3*, and *Ryr2* was performed in the Cepheid SmartCycler II, using reagents from PCR Core System I (Promega). Succinate dehydrogenase complex subunit A (*SDHA*) was chosen as the internal control gene for normalization. *SDHA* has previously shown high expression stability in pooled human heart tissue (64). Furthermore, *SDHA* demonstrated similar abundance as the three target genes in murine cardiac tissue. Each real-time PCR reaction was performed in duplicate;

negative control PCR reactions were included with each assay to ensure the absence of template contamination in PCR reagents.

Amplification products generated during real-time PCR were detected through intercalation of the fluorescent dye SYBR Green I (Molecular Probes). SYBR Green binds nonspecifically to all double-stranded DNA. Therefore, measures were taken to minimize formation of undesired PCR products. Net Primer software (Premier Biosoft International) was used in conjunction with Primer 3 software (Whitehead Institute) to minimize formation of primer dimer products. A rodent mispriming library was also utilized by the Primer 3 software to minimize the formation of mispriming products. Primer pairs were designed to recognize cDNA generated from *Tnnt2*, *Tnni3*, *Ryr2*, and *SDHA* mRNA. To ensure primer specificity for cDNA, with no recognition of genomic DNA, one primer from each pair was designed to span an exon-exon junction.

All primers were designed to contain twenty nucleotides and 50% G + C composition. The PCR products generated by each primer pair were analogous in size, ranging from 187-204 nucleotides in length. Table 4 lists the nucleotide sequences of the primers, the length of PCR products generated by each primer pair, and the T_m values of the PCR products. Each primer pair was confirmed to generate the desired PCR product through PAGE analysis of RT-PCR products from adult cardiac RNA. As with every PCR reaction performed in this study, negative control reactions were included to ensure the absence of template contamination in PCR reagents. During real-time PCR optimization, the generation of desired PCR products was once again confirmed through PAGE analysis. T_m values were used for subsequent identification of desired PCR products in real-time PCR.

Table 4. Primer pairs designed for cDNA amplification.

Primer	Sequence (5'→3')	Length of PCR product (bp)	T_m of PCR product (°C)
Troponin T2-L	AACGTAGAAGAGGTTGGTCC	190	88.96
Troponin T2-R	TCTGTAGCTCATTCAGGTCC		
Troponin I-L	CCACACGCCAAGAAAAAGTC	204	89.68
Troponin I-R	AAGCTGTCGGCATAAGTCCT		
Ryanodine Receptor 2-L	ATGTCCAAGGCAGCCATTTC	197	87.47
Ryanodine Receptor 2-R	TCCTCCTCGGTGTCTTTCAA		
SDHA-L	GTCAGCTCTATGGAGACCTA	187	89.12
SDHA-R	TCGACCCGCACTTTGTAATC		

Real-time PCR reaction conditions were optimized prior to data collection for each primer pair. Reagent concentrations (Sybr Green, $MgCl_2$) were optimized, in addition to cycling parameters (annealing temperature, duration of cycling steps). The optimum $MgCl_2$ concentrations for *Tnnt2*, *Tnni3*, *RyR2*, and *SDHA* primer pairs were 2mM, 5mM, 3mM, and 3mM, respectively. Each real-time PCR reaction mixture was assembled on wet ice, as shown in Table 5.

Table 5. Real-time PCR reaction components.

Component	µL/reaction	[stock]	[final]
H_20	variable	n/a	n/a
$MgCl_2$	variable	25 mM	variable
Reaction Buffer	2.5	10 x	1 x
dNTPs	0.5	10 mM each	0.2 mM each
Sybr Green	0.125	100 x	0.5 x
Taq DNA Polymerase	0.25	5 u/µl	2.5 u/µg cDNA
Primer-L	5	2.5 µM	0.5µM
Primer-R	5	2.5 µM	0.5µM
cDNA	5	100 ng/µl	20 ng/µl
Total Reaction Volume	25		

The optimum annealing temperatures for *Tnnt2*, *Tnni3*, *RyR2*, and *SDHA* primer pairs were 60°C, 57 °C, 60 °C, and 65 °C, respectively. The cycling parameters utilized for real-time PCR are displayed in Table 6. Following initial denaturation, the three temperature steps (denaturation, annealing, and extension) were repeated a maximum of 30 times, or until C_T was reached. The fluorescence threshold was set at 30.0 for each assay. A melt curve was generated immediately after C_T was reached; the melting curve started at 60.0 °C and ended at 95.0 °C, increasing 0.2 °C per second. If the T_m of the desired PCR product was not identified with the melt curve, then the corresponding C_T value was omitted from the data set.

Table 6. Real-time PCR cycling parameters.

Stage	No. cycles	Temp (°C)	Time (sec)	Optics
1	1	95.0 °C	60	Off
2	Maximum of 30	95.0 °C	15	Off
		Variable	30	Off
		72.0 °C	30	On
3	1	60 °C - 95 °C	175	Off

Statistical Analysis

The arithmetic mean and standard deviation were calculated for C_T values from duplicate reactions. The relative levels of *Tnnt2*, *Tnni3*, and *Ryr2* were then determined through normalization to *SDHA* transcript levels, using the arithmetic formula $2^{-\Delta Ct}$. For each assay, ΔC_T was calculated by subtracting the mean C_T value for the reference gene (*SDHA*) from the mean C_T value of the target gene (*Tnnt2*, *Tnni3*, or *Ryr2*). The $2^{-\Delta Ct}$ value generated represented the fold difference in gene expression between the target and reference gene. Since the reference gene should be constitutively expressed, differences in $2^{-\Delta Ct}$ values should solely represent changes in target gene expression levels.

Statistical analyses of the data from each MPKU litter (maternal blood Phe concentration and relative abundance of *Tnnt2*, *Tnni3*, and *Ryr2* transcripts) were performed using the SAS System (The SAS System for Windows NT, version 5.1.2600, copyright 1999-2000 by SAS Institute Inc., Cary NC, USA). Descriptive statistics were generated to ensure normal distribution of maternal blood Phe levels. Linear regression analysis was then performed on the relative transcript levels of *Tnnt2*, *Tnni3*, and *Ryr2* as a function of maternal blood Phe concentration. Log transformation of the data was subsequently performed; regression analyses were repeated with the transformed data set to evaluate the best-fit model by comparison of r^2 values. Regression analyses were also performed on the relative transcript levels of *Tnnt2*, *Tnni3*, and *Ryr2* levels as a function of tissue storage length. This was done to determine whether variations in tissue storage time affected cardiac transcript levels.

RESULTS

Data Analysis

Linear regression analyses were nonsignificant for *Tnnt2* ($F = 0.09$; d.f. = 1, 31; $p = 0.7640$), *Tnni3* ($F = 0.55$; d.f. = 1, 31; $p = 0.4642$), and *RyR2* ($F = 1.57$; d.f. = 1, 31; $p = 0.2200$) transcript levels as a function of maternal blood Phe concentration. The data plots for *Tnnt2*, *Tnni3*, and *RyR2* are illustrated in Figures 1-3, respectively. Log transformation of the data sets and subsequent regression analyses did not change the outcome of nonsignificance. Regression analyses were also nonsignificant for *Tnnt2* ($F = 3.55$; d.f. = 1, 31; $p = 0.0688$), *Tnni3* ($F = 0.09$; d.f. = 1, 31; $p = 0.7643$), and *RyR2* ($F = 2.23$; d.f. = 1, 31; $p = 0.1451$) transcript levels as a function of tissue storage length at -80^{o}C.

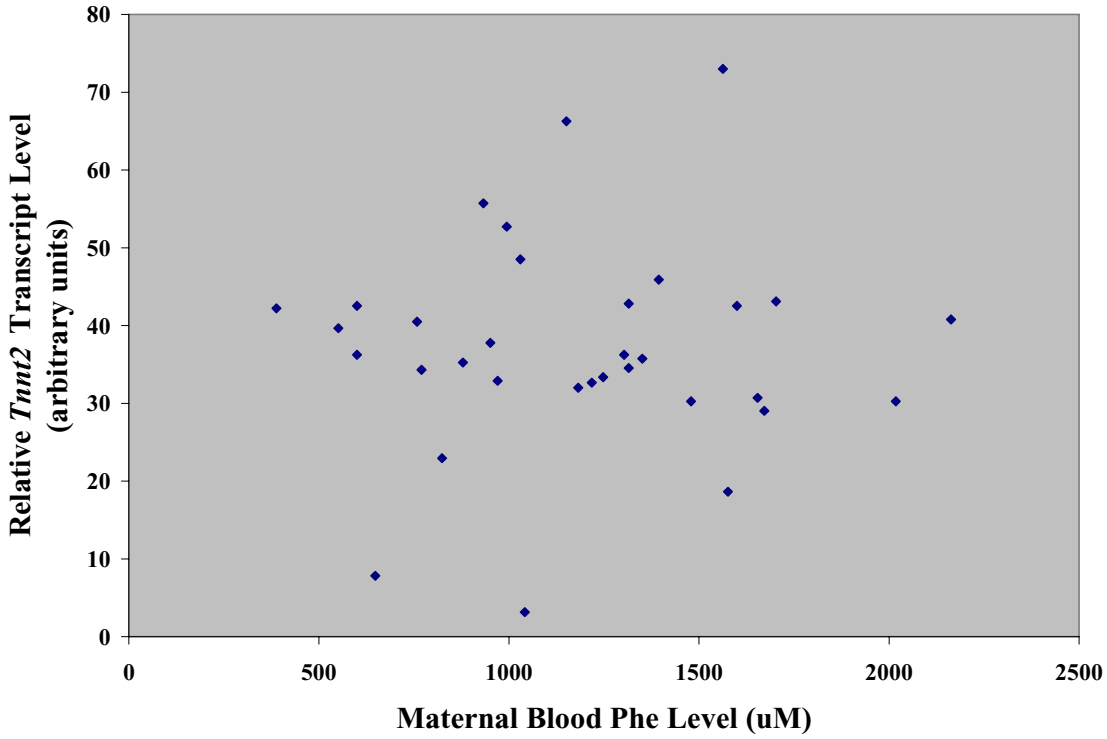

Figure 3. Relative *Tnnt2* transcript levels in MPKU fetal hearts versus maternal blood phenylalanine levels.

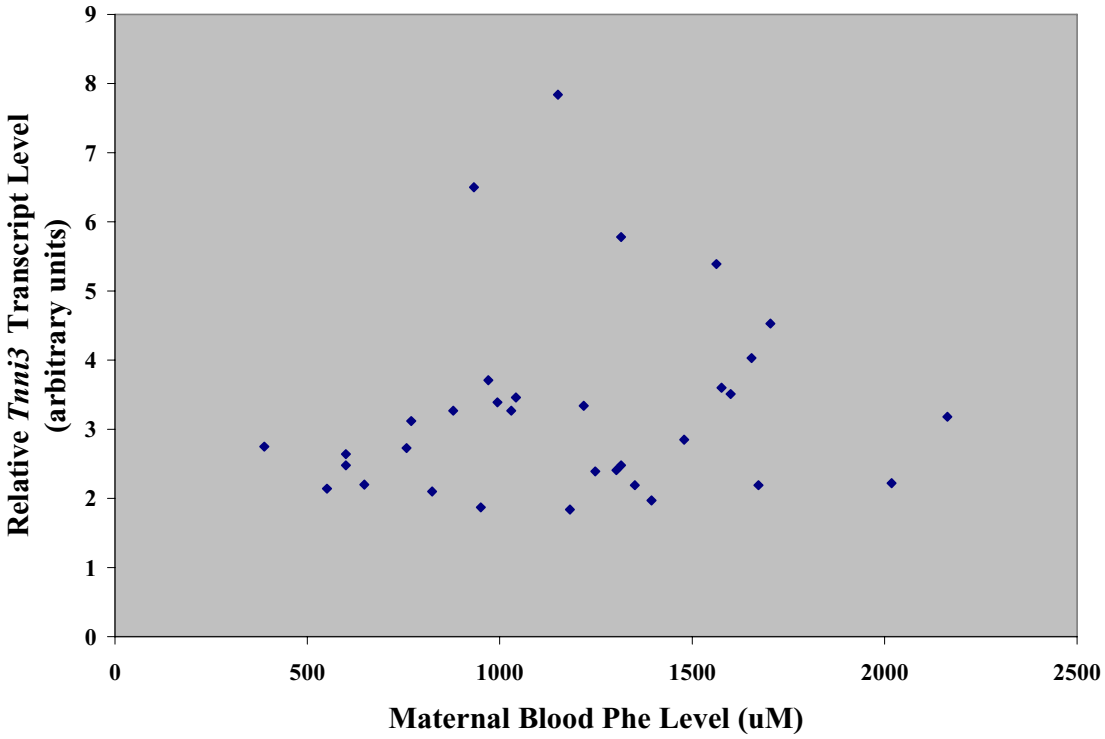

Figure 4. Relative *Tnni3* transcript levels in MPKU fetal hearts versus maternal blood phenylalanine levels.

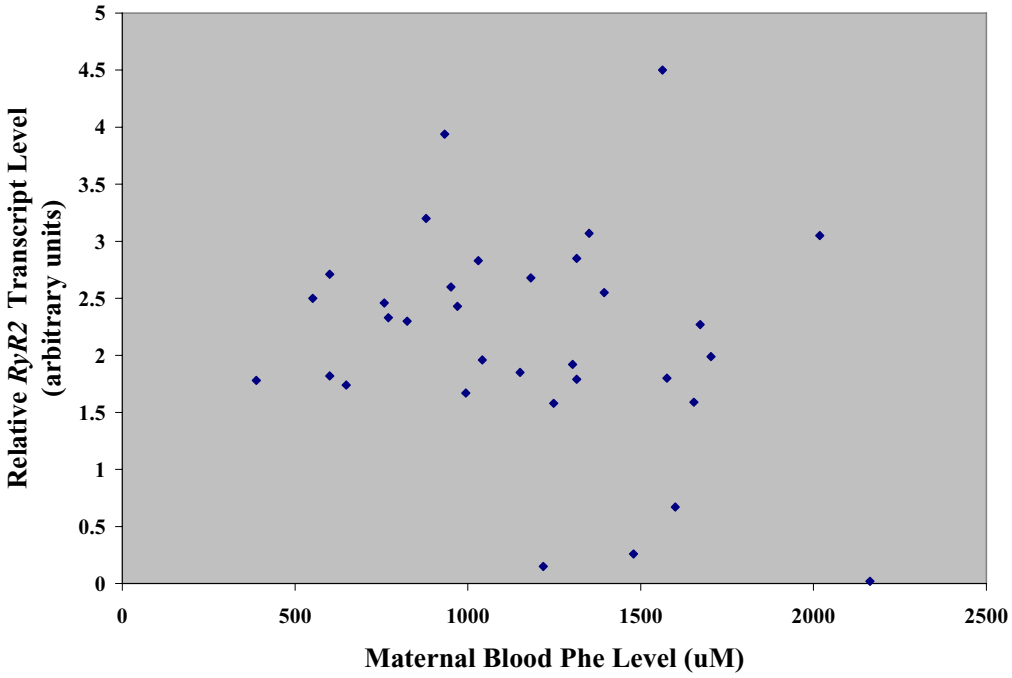

Figure 5. Relative *RyR2* transcript levels in MPKU fetal hearts versus maternal blood phenylalanine levels.

DISCUSSION

Implications of Results

The null hypothesis stated no association between maternal blood Phe concentrations and the abundance of *Tnnt2*, *Tnni3*, and *Ryr2* transcripts in MPKU fetal hearts. Since the regression analyses were nonsignificant for all three genes tested, we were unable to reject the null hypothesis. This implies no association between maternal blood Phe concentrations and the abundance of *Tnnt2*, *Tnni3*, and *Ryr2* transcripts in MPKU fetal hearts.

The length of tissue storage prior to heart isolation varied from sample to sample. A regression analysis was performed to determine whether the abundance of cardiac transcripts was affected by the length of tissue storage. There was a near significant ($p = 0.0688$), slight decrease in *Tnnt2* transcript levels as the length of tissue storage increased. Although this small effect was seen with storage time, it was not significant enough to mask a dose-response relationship between maternal blood Phe concentration and transcript abundance.

Experimental Limitations

In previous MPKU studies using the BTBR-*Pah*^{enu2} mouse model, maternal blood Phe concentrations were modulated by combining a Phe-deficient synthetic diet with various concentrations of Phe supplementation in the drinking water. This method successfully produced the range of maternal blood Phe concentrations necessary for evaluating dose-response relationships. The maternal blood Phe levels ranged from normal (<200 μM) to severely high (>1,200 μM) using this method.

During this MPKU study, maternal blood Phe concentrations were modulated using the LNAA dietary supplement. The mean maternal blood Phe levels produced within each LNAA treatment group are shown in Figure 6. In human MPKU, maternal blood Phe levels are considered to be under strict metabolic control when maintained lower than 600 μM throughout pregnancy; this reduces the risk of MPKU congenital heart defects from 14% to 6% (18, 20). Using LNAA supplementation, only 2 of the 33 MPKU females in this study exhibited maternal blood Phe levels lower than 600 μM.

The 16.7% and 20.0% LNAA groups did not show significant reductions in maternal blood Phe concentrations compared to the 0% LNAA supplementation group. The 33.4% LNAA group did show significant reductions in maternal blood Phe levels compared to the 0% LNAA group; however, these reductions were not dramatic enough to produce normal blood Phe concentrations in most MPKU pregnancies. Therefore, LNAA supplementation did not adequately normalize maternal blood Phe concentrations for a robust MPKU dose-response study.

The transcript levels of the three target genes were normalized using the internal control gene *SDHA*. Originally, three internal control genes were chosen for this study: glyceraldehyde-3-phosphate dehydrogenase (*GAPDH*), hydroxymethyl-bilane synthase (*HMBS*), and *SDHA*. The use of multiple control genes provides more reliable normalization factors than those generated from one control gene alone (64). *GAPDH*, *HMBS*, and *SDHA* were chosen due to their documented expression stability in adult human heart tissue. Furthermore, these genes had similar abundance levels in murine fetal cardiac tissue as the three target genes.

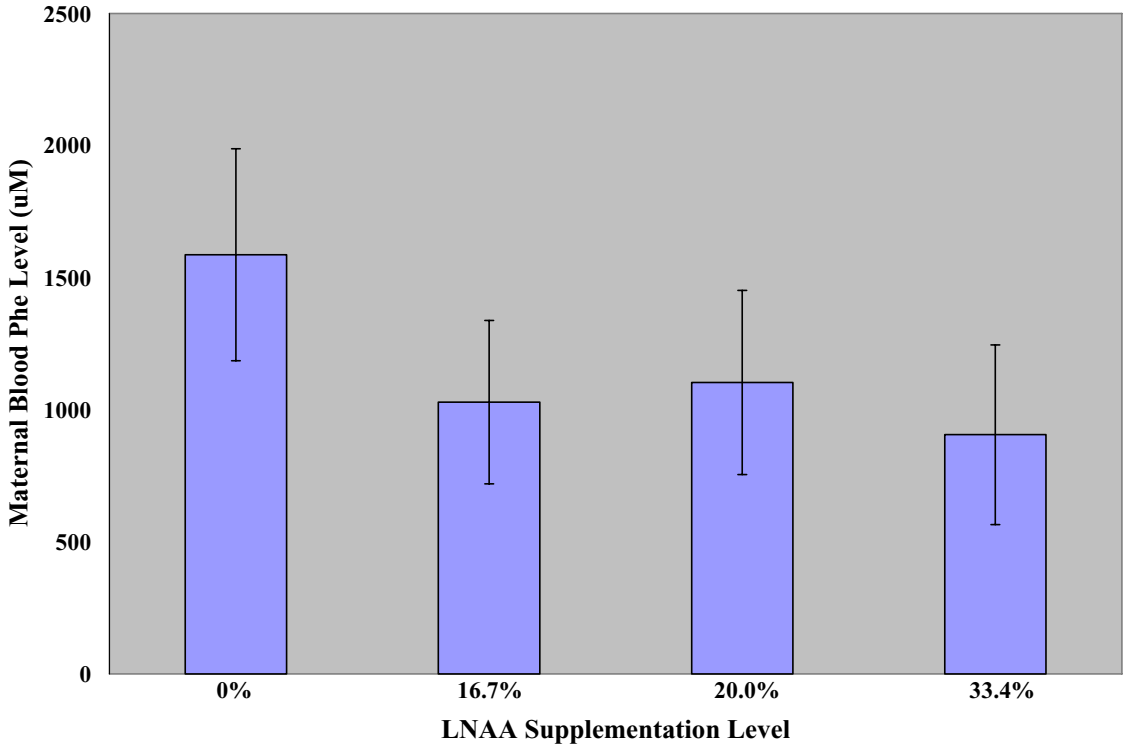

Figure 6. Mean maternal blood phenylalanine levels (±1 SD) produced using LNAA supplementation.

Primer pairs were created to recognize cDNA from *GAPDH*, *HMBS*, and *SDHA*. All primer pairs were designed specifically to minimize formation of primer dimer products during real-time PCR. Nevertheless, the *HMBS* primers consistently created undesired products; for this reason, *HMBS* was omitted from the study. C_T values for *GAPDH* and *SDHA* were determined during each real-time PCR assay, and the geometric mean of these two internal control genes was calculated for normalization of target gene abundance.

An ideal internal control gene is constitutively expressed, regardless of experimental treatment; therefore, internal control genes should not vary significantly in abundance among the samples tested. To compare the extent of statistical variation in *GAPDH* and *SDHA* among samples, coefficients of variation (CV) were calculated. The expression of SDHA varied 3% on average between samples, while GAPDH varied 6% on average between samples. Since *GAPDH* expression fluctuated twice as much as *SDHA* expression, *SDHA* alone was used to normalize the transcript levels of the three target genes.

For relative quantification assays, it is essential to identify the most stably expressed control genes in a given tissue type. Ideally, the presumed expression stability of an internal control gene should be validated prior to experimentation. However, variations in mRNA levels can result from sources other than expression instability. For instance, resuspension of RNA based on total RNA quantity might have contributed to fluctuations in mRNA levels between samples. This is because total RNA consists predominantly of rRNA, not mRNA. Resuspension of total RNA based on original tissue

weight (or ideally, the original number of cells) might have minimized some of these fluctuations.

Future Directions

The heart is the only fetal organ other than the brain known to be affected by MPKU (65). While greater than 90% of offspring from untreated human MPKU pregnancies suffer microcephaly and mental retardation (57), congenital hearts defects only occur in 14% of untreated MPKU offspring (19). A dose-response relationship has been established between maternal hyperphenylalaninemia and microcephaly (18). However, the precise relationship between hyperphenylalaninemia and the development of congenital heart defects still needs to be elucidated. It is possible that a threshold of maternal hyperphenylalaninemia must be reached during critical stages of heart development for subsequent pathogenesis. However, as with other MPKU birth defects, a dose-response relationship could exist. Furthermore, hyperphenylalaninemia might not be the only factor involved in the development of MPKU heart defects.

In future studies, it would be beneficial to evaluate the molecular basis of MPKU congenital heart defects at earlier developmental stages. It has already been established that *Tnnt2*, *Tnni3*, and *Ryr2* are significantly downregulated in the hearts of 18.5 dpc MPKU offspring compared to non-PKU control offspring (27). However, the majority of heart development has already occurred by this stage. It is likely that abnormal cardiac gene expression at 18.5 dpc results from earlier aberrations in gene expression. Cardiac transcription factors (such as bone morphogenic proteins, fibroblast growth factors, and homeobox proteins) are likely candidates for analysis at earlier stages of heart development. Once the molecular basis of congenital heart defects has been elucidated

at earlier stages of heart morphogenesis, researchers will be better equipped to determine the mechanism linking hyperphenylalaninemia to cardiac pathogenesis.

LIST OF REFERENCES

1. Zellweger H 1961 Aminoaciduria and mental retardation. II. Phenylpyruvic oligophrenia, phenylketonuria (PKU). J Iowa State Med Soc 51:536-540

2. Waisbren SE, Hanley W, Levy HL, Shifrin H, Allred E, Azen C, Chang PN, Cipcic-Schmidt S, de la Cruz F, Hall R, Matalon R, Nanson J, Rouse B, Trefz F, Koch R 2000 Outcome at age 4 years in offspring of women with maternal phenylketonuria: the Maternal PKU Collaborative Study. Jama 283:756-762

3. Paine RS 1957 The variability in manifestations of untreated patients with phenylketonuria (phenylpyruvic aciduria). Pediatrics 20:290-302

4. Lidsky AS, Law ML, Morse HG, Kao FT, Rabin M, Ruddle FH, Woo SL 1985 Regional mapping of the phenylalanine hydroxylase gene and the phenylketonuria locus in the human genome. Proc Natl Acad Sci U S A 82:6221-6225

5. Guttler F, Woo SL 1986 Molecular genetics of PKU. J Inherit Metab Dis 9 Suppl 1:58-68

6. Burgard P, Rupp A, Konecki DS, Trefz FK, Schmidt H, Lichter-Konecki U 1996 Phenylalanine hydroxylase genotypes, predicted residual enzyme activity and phenotypic parameters of diagnosis and treatment of phenylketonuria. Eur J Pediatr 155 Suppl 1:S11-15

7. Gregory DM, Sovetts D, Clow CL, Scriver CR 1986 Plasma free amino acid values in normal children and adolescents. Metabolism 35:967-969

8. Scriver CR, Gregory DM, Sovetts D, Tissenbaum G 1985 Normal plasma free amino acid values in adults: the influence of some common physiological variables. Metabolism 34:868-873

9. McKean CM, Boggs DE, Peterson NA 1968 The influence of high phenylalanine and tyrosine on the concentrations of essential amino acids in brain. J Neurochem 15:235-241

10. Hommes FA, Lee JS 1990 The control of 5-hydroxytryptamine and dopamine synthesis in the brain: a theoretical approach. J Inherit Metab Dis 13:37-57

11. Woolf LI, Vulliamy DG 1951 Phenylketonuria with a study of the effect upon it of glutamic acid. Arch Dis Child 26:487-494

12. Armstrong MD, Tyler FH 1955 Studies on phenylketonuria. I. Restricted phenylalanine intake in phenylketonuria. J Clin Invest 34:565-580

13. Bickel H, Gerrard J, Hickmans EM 1954 The influence of phenylalanine intake on the chemistry and behaviour of a phenyl-ketonuric child. Acta Paediatr 43:64-77

14. Woolf LI, Griffiths R, Moncrieff A 1955 Treatment of phenylketonuria with a diet low in phenylalanine. Br Med J 4905:57-64

15. Rohr FJ, Doherty LB, Waisbren SE, Bailey IV, Ampola MG, Benacerraf B, Levy HL 1987 New England Maternal PKU Project: prospective study of untreated and treated pregnancies and their outcomes. J Pediatr 110:391-398

16. Koch R, Levy H, Hanley W, Matalon R, Rouse B, Trefz F, de la Cruz F 1996 Outcome implications of the International Maternal Phenylketonuria Collaborative Study (MPKUCS): 1994. Eur J Pediatr 155 Suppl 1:S162-164

17. Lenke RR, Levy HL 1980 Maternal phenylketonuria and hyperphenylalaninemia. An international survey of the outcome of untreated and treated pregnancies. N Engl J Med 303:1202-1208

18. Rouse B, Azen C, Koch R, Matalon R, Hanley W, de la Cruz F, Trefz F, Friedman E, Shifrin H 1997 Maternal Phenylketonuria Collaborative Study (MPKUCS) offspring: facial anomalies, malformations, and early neurological sequelae. Am J Med Genet 69:89-95

19. Levy HL, Guldberg P, Guttler F, Hanley WB, Matalon R, Rouse BM, Trefz F, Azen C, Allred EN, de la Cruz F, Koch R 2001 Congenital heart disease in maternal phenylketonuria: report from the Maternal PKU Collaborative Study. Pediatr Res 49:636-642

20. Ghavami M, Levy HL, Erbe RW 1986 Prevention of fetal damage through dietary control of maternal hyperphenylalaninemia. Clin Obstet Gynecol 29:580-585

21. Mitchell SC, Korones SB, Berendes HW 1971 Congenital heart disease in 56,109 births. Incidence and natural history. Circulation 43:323-332

22. Shedlovsky A, McDonald JD, Symula D, Dove WF 1993 Mouse models of human phenylketonuria. Genetics 134:1205-1210

23. McDonald JD, Charlton CK 1997 Characterization of mutations at the mouse phenylalanine hydroxylase locus. Genomics 39:402-405

24. Zagreda L, Goodman J, Druin DP, McDonald D, Diamond A 1999 Cognitive deficits in a genetic mouse model of the most common biochemical cause of human mental retardation. J Neurosci 19:6175-6182

25. Cho S, McDonald JD 2001 Effect of maternal blood phenylalanine level on mouse maternal phenylketonuria offspring. Mol Genet Metab 74:420-425

26. McDonald JD, Dyer CA, Gailis L, Kirby ML 1997 Cardiovascular defects among the progeny of mouse phenylketonuria females. Pediatr Res 42:103-107

27. Surendran S, Okorodudu, A.O., Campbell, G.A., Tyring, S.K., Michals-Matalon, K., McDonald, J.D. and Matalon, R. 2005 Abnormal Expression of Genes Associated with Development and Inflammation in the Heart of Mouse Maternal Phenylketonuria Offspring. In press for International Journal of Immunopathology and Pharmacology

28. Wessels A, Sedmera D 2003 Developmental anatomy of the heart: a tale of mice and man. Physiol Genomics 15:165-176

29. Bruneau BG 2002 Transcriptional regulation of vertebrate cardiac morphogenesis. Circ Res 90:509-519

30. Srivastava D, Olson EN 2000 A genetic blueprint for cardiac development. Nature 407:221-226

31. Bartman T, Hove J 2005 Mechanics and function in heart morphogenesis. Dev Dyn 233:373-381

32. Chen JN, Haffter P, Odenthal J, Vogelsang E, Brand M, van Eeden FJ, Furutani-Seiki M, Granato M, Hammerschmidt M, Heisenberg CP, Jiang YJ, Kane DA, Kelsh RN, Mullins MC, Nusslein-Volhard C 1996 Mutations affecting the cardiovascular system and other internal organs in zebrafish. Development 123:293-302

33. Stainier DY, Fouquet B, Chen JN, Warren KS, Weinstein BM, Meiler SE, Mohideen MA, Neuhauss SC, Solnica-Krezel L, Schier AF, Zwartkruis F, Stemple DL, Malicki J, Driever W, Fishman MC 1996 Mutations affecting the formation and function of the cardiovascular system in the zebrafish embryo. Development 123:285-292

34. Sehnert AJ, Huq A, Weinstein BM, Walker C, Fishman M, Stainier DY 2002 Cardiac troponin T is essential in sarcomere assembly and cardiac contractility. Nat Genet 31:106-110

35. Greaser ML, Gergely J, Han MH, Benson ES 1972 Lack of identity of tropocalcin with troponin components. Biochem Biophys Res Commun 48:358-361

36. Solaro RJ, Rarick HM 1998 Troponin and tropomyosin: proteins that switch on and tune in the activity of cardiac myofilaments. Circ Res 83:471-480

37. Sia SK, Li MX, Spyracopoulos L, Gagne SM, Liu W, Putkey JA, Sykes BD 1997 Structure of cardiac muscle troponin C unexpectedly reveals a closed regulatory domain. J Biol Chem 272:18216-18221

38. Adamcova M, Pelouch V 1999 Isoforms of troponin in normal and diseased myocardium. Physiol Res 48:235-247

39. Malhotra A, Nakouzi A, Bowman J, Buttrick P 1997 Expression and regulation of mutant forms of cardiac TnI in a reconstituted actomyosin system: role of kinase dependent phosphorylation. Mol Cell Biochem 170:99-107

40. Swiderek K, Jaquet K, Meyer HE, Schachtele C, Hofmann F, Heilmeyer LM, Jr. 1990 Sites phosphorylated in bovine cardiac troponin T and I. Characterization by 31P-NMR spectroscopy and phosphorylation by protein kinases. Eur J Biochem 190:575-582

41. Chen Z, Higashiyama A, Yaku H, Bell S, Fabian J, Watkins MW, Schneider DJ, Maughan DW, LeWinter MM 1997 Altered expression of troponin T isoforms in mild left ventricular hypertrophy in the rabbit. J Mol Cell Cardiol 29:2345-2354

42. Pearlstone JR, Carpenter MR, Smillie LB 1986 Amino acid sequence of rabbit cardiac troponin T. J Biol Chem 261:16795-16810

43. Wilkinson JM, Grand RJ 1978 Comparison of amino acid sequence of troponin I from different striated muscles. Nature 271:31-35

44. Brenner B 1991 A new concept for the mechanism of Ca+(+)-regulation of muscle contraction. Implications for physiological and pharmacological approaches to modulate contractile function of myocardium. Basic Res Cardiol 86 Suppl 3:83-92

45. Anderson PA, Greig A, Mark TM, Malouf NN, Oakeley AE, Ungerleider RM, Allen PD, Kay BK 1995 Molecular basis of human cardiac troponin T isoforms expressed in the developing, adult, and failing heart. Circ Res 76:681-686

46. Toyota N, Shimada Y 1981 Differentiation of troponin in cardiac and skeletal muscles in chicken embryos as studied by immunofluorescence microscopy. J Cell Biol 91:497-504

47. Moolman JC, Corfield VA, Posen B, Ngumbela K, Seidman C, Brink PA, Watkins H 1997 Sudden death due to troponin T mutations. J Am Coll Cardiol 29:549-555

48. Ertz-Berger BR, He H, Dowell C, Factor SM, Haim TE, Nunez S, Schwartz SD, Ingwall JS, Tardiff JC 2005 Changes in the chemical and dynamic properties of cardiac troponin T cause discrete cardiomyopathies in transgenic mice. Proc Natl Acad Sci U S A 102:18219-18224

49. Huang X, Pi Y, Lee KJ, Henkel AS, Gregg RG, Powers PA, Walker JW 1999 Cardiac troponin I gene knockout: a mouse model of myocardial troponin I deficiency. Circ Res 84:1-8

50. Otsu K, Fujii J, Periasamy M, Difilippantonio M, Uppender M, Ward DC, MacLennan DH 1993 Chromosome mapping of five human cardiac and skeletal muscle sarcoplasmic reticulum protein genes. Genomics 17:507-509

51. Tiso N, Stephan DA, Nava A, Bagattin A, Devaney JM, Stanchi F, Larderet G, Brahmbhatt B, Brown K, Bauce B, Muriago M, Basso C, Thiene G, Danieli GA, Rampazzo A 2001 Identification of mutations in the cardiac ryanodine receptor gene in families affected with arrhythmogenic right ventricular cardiomyopathy type 2 (ARVD2). Hum Mol Genet 10:189-194

52. Tunwell RE, Wickenden C, Bertrand BM, Shevchenko VI, Walsh MB, Allen PD, Lai FA 1996 The human cardiac muscle ryanodine receptor-calcium release channel: identification, primary structure and topological analysis. Biochem J 318 (Pt 2):477-487

53. Fabiato A, Fabiato F 1978 Calcium-induced release of calcium from the sarcoplasmic reticulum of skinned cells from adult human, dog, cat, rabbit, rat, and frog hearts and from fetal and new-born rat ventricles. Ann N Y Acad Sci 307:491-522

54. Korzick DH 2003 Regulation of cardiac excitation-contraction coupling: a cellular update. Adv Physiol Educ 27:192-200

55. Takeshima H, Komazaki S, Hirose K, Nishi M, Noda T, Iino M 1998 Embryonic lethality and abnormal cardiac myocytes in mice lacking ryanodine receptor type 2. Embo J 17:3309-3316

56. Leenhardt A, Lucet V, Denjoy I, Grau F, Ngoc DD, Coumel P 1995 Catecholaminergic polymorphic ventricular tachycardia in children. A 7-year follow-up of 21 patients. Circulation 91:1512-1519

57. Levy HL, Ghavami M 1996 Maternal phenylketonuria: a metabolic teratogen. Teratology 53:176-184

58. Rouse B, Matalon R, Koch R, Azen C, Levy H, Hanley W, Trefz F, de la Cruz F 2000 Maternal phenylketonuria syndrome: congenital heart defects, microcephaly, and developmental outcomes. J Pediatr 136:57-61

59. Matalon R, Surendran S, Matalon KM, Tyring S, Quast M, Jinga W, Ezell E, Szucs S 2003 Future role of large neutral amino acids in transport of phenylalanine into the brain. Pediatrics 112:1570-1574

60. McCaman MWaR, E. 1962 Fluorometric method for determination of phenylalanine in serum. J Lab Clin Med 59:885-890

61. Wu JT, Wu LH, Ziter FA, Ash KO 1979 Manual fluorometry of phenylalanine from blood specimens collected on filter paper: a modified procedure. Clin Chem 25:470-472

62. Chomczynski P 1993 A reagent for the single-step simultaneous isolation of RNA, DNA and proteins from cell and tissue samples. Biotechniques 15:532-534, 536-537

63. Freeman WM, Walker SJ, Vrana KE 1999 Quantitative RT-PCR: pitfalls and potential. Biotechniques 26:112-122, 124-115

64. Vandesompele J, De Preter K, Pattyn F, Poppe B, Van Roy N, De Paepe A, Speleman F 2002 Accurate normalization of real-time quantitative RT-PCR data by geometric averaging of multiple internal control genes. Genome Biol 3:RESEARCH0034.1-0034.12

65. Brenton DP 1990 Cardiac defects in the children of mothers with high concentrations of plasma phenylalanine. Br Heart J 63:143-144